Nuclear Engineering and Technology 52 (2020) 1164–1171

Contents lists available at ScienceDirect

Nuclear Engineering and Technology

journal homepage: www.elsevier.com/locate/net

Original Article

Liquid entrainment through a large-scale inclined branch pipe on a horizontal main pipe

Ningxin Gu [a], Geyu Shen [a], Zhiyuan Lu [a], Yuenan Yang [b], Zhaoming Meng [a, *], Ming Ding [a, **]

[a] Fundamental Science on Nuclear Safety and Simulation Technology Laboratory, Harbin Engineering University, Harbin, Heilongjiang, 150001, China
[b] Patent Examination Cooperation (Beijing) Center of the Patent Office, SIPO, China

ARTICLE INFO

Article history:
Received 8 November 2018
Received in revised form
8 October 2019
Accepted 6 November 2019
Available online 8 November 2019

Keywords:
Inclined T-junction
Large-scale
Liquid entrainment

ABSTRACT

T-junction structures play an important role in nuclear power plant systems. Research on liquid entrainment is mostly based on small-scale branch pipes (d/D $\leq$ 0.2) and attention paid to large-scale branch pipes (0.33 < d/D < 1) is insufficient. Accordingly, this study implements a series of experiments on the liquid entrainment of T-junction with different angles (32.2°,47.9°,62.3°,90°) through a large-scale branch (d/D = 0.675).The onset liquid entrainment is related to the gas phase Froude number Fr_g, the dimensionless gas chamber height h_b/d and the branch pipe angle θ. As Fr_g increases, h_b/d also rises. With a constant h_b/d, the onset liquid entrainment changes from droplets entrainment by the gas phase to that by the rising liquid film. The steady-state liquid entrainment is related to w_{3g}, h/d and θ. With constant w_{3g} and h/d, the branch quality grows as the branch angle increases. With a certain h/d, the branch quality increases, as the w_{3g} number increases.

1. Introduction

T-junction structures have been essential in many industrial applications, especially those in nuclear power plant. Examples include those T-junctions installed between header and feeder pipes in CANDU (Canadian Deuterium Uranium) reactor [1], the joints between hot leg and ADS-4 (Fourth Stage Automatic Depressurization System) pipelines [2], PRHRS (Passive Residual Heat Removal System) pipelines, the flow through a small break in a horizontal channel of a nuclear power plant during LOCA (Loss of Coolant Accident) [3]. In the case with a two-phase stratified flow in the horizontal main pipe of T-junction, the liquid phase can be entrained into the branch pipe by the gas phase [4]. This process may occur at T-junctions during LOCA which can directly lead to reduction of water inventory in the reactor core, thus affecting reactor safety. Therefore, it is critical to properly predict possible liquid entrainment phenomenon in order to ensure safety of the nuclear power plant.

In 1956, Rouse et al. [5] was the first researcher to study the mechanism of liquid entrainment. In 1980, Zuber [4] pointed out that liquid entrainment may occur at the break in the coolant loss accident. Crowley et al. [6] carried out a series of visual experiments with air-water in 1981 and the experimental data were compared with the onset entrainment model developed by Rouse, the model was in good agreement with the experimental data. During last several decades, attention has been paid to entrainment issues. Realizing their importance, Welter [7] argues the efficiency of available computer codes in satisfactorily predicting either the amount or onset of liquid entrainment that was generally accompanied with large break in the horizontal coolant pipe. Correspondingly, this study aims to explore influencing factors of liquid entrainment at T-junction through the large branch with certain angles (32.2°,47.9°,62.3°,90°), results of which are expected to provide references for nuclear power plant safety analysis and enrich programs for relevant calculation.

Entrainment models developed for small branch pipes or minor breaks of certain angles have been extensively applied to RELAP5 program [7–9], which are accompanied with proper prediction of entrainment behaviors. As shown in Table 1, the onset of liquid entrainment is closely related to the branch angle, during which vortex or rising liquid film can be observed.

As shown in Fig. 1, which was reproduced from Lee et al. [9], for a given gas flow, as the liquid level increases, a weak entrainment

* Corresponding author.
** Corresponding author.
E-mail address: mengzhaoming@hrbeu.edu.cn (Z. Meng).

https://doi.org/10.1016/j.net.2019.11.009

Table 1
Onset mechanism of liquid entrainment at branch pipes with certain angles.

Entrainment starting point	Liquid-phase entrainment	
Direction of branch pipes	Upward	Horizontal/Slant
Entrainment mechanism	Vortex	Rising liquid film

with vortex is observed below branch entrance (Fig. 1(a)). The droplets which separated from the end of the entrained crest, is deposited on the inner wall of the horizontal pipe. As a further increase of liquid level, the entrained liquid reaches the entrance of branch (Fig. 1(b)), which is defined as OLE (onset liquid entrainment) at top branches. For the vertical upward branch, liquid entrainment begins as droplets jump into the branch, as shown in Fig. 1(c). For the incline branch, as a given gas flow, the liquid film starts to arise as shown in Fig. 1(d). With further increase of the liquid level, droplets appear on the inner wall of the branch pipe (Fig. 1(e)). Finally, a thin rising film of water which enters into the branch determines the onset of liquid entrainment (Fig. 1(f)).

Inclined branch pipes with angles of $+36^\circ$ are demonstrated to disfavor swirling entrainment due to friction of main pipe inner walls [10,11]. Liquid entrainment in the $+36^\circ$ branch pipe is similar to that in the horizontal branch pipe, whereas that in $+72^\circ$ branch pipe is similar to that of vertically upward branch pipes.

As shown in Table 2, mechanisms of liquid entrainment in small branch pipes have been well elaborated. However, insufficient attention has been paid to entrainment in large branch pipes, especially by visualization means.

According to hypothesis of inertia force and gravitational equilibrium of two-phase interfaces on the onset of entrainment, occurrence of vortex or rising liquid film is thought to represent the onset of entrainment. Given the influence of branch pipe angle on entrainment, a semi-empirical entrainment onset model was built [14], which regarded vortex occurrence as onset of liquid entrainment:

$$Frg\left(\frac{\rho g}{\Delta\rho}\right)^{0.5} = C_{b(\theta)}\left[\left(\frac{hb}{d}\right) + \frac{1}{2}\left(\frac{D}{d}\right)(1-\sin\theta)\right]^{2.5} \tag{1}$$

Another model that regards occurrence of rising liquid film as onset of liquid entrainment is shown as follows:

$$Frg\left(\frac{\rho g}{\Delta\rho}\right)^{0.5} = C_{b(\theta=0)}\left(\frac{hb}{d}\right)^{2.5} \tag{2}$$

where g stands for gas phase and θ means the included angle between branch pipe and horizontal direction.

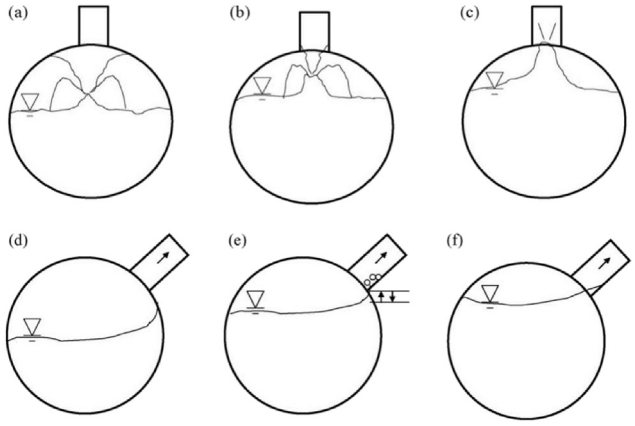

Fig. 1. Two forms of onset liquid entrainment [9].

This model can predict liquid entrainment initiation points at any angle to a certain extent. However, the coefficient, which is branch pipe angle dependent, needs to be experimentally determined. Besides, as for liquid-phase entrainment, Eq. (2) is only applicable to the range of angles that are used for coefficient determination.

In view of the possible entrainment in the AP600 nuclear power plant, Welter et al. [7,16] established a one-dimensional steady-state manifold mass gas content model:

$$x = \frac{1}{1 + W3l/W3g} \tag{3}$$

Among them,

$$\frac{W3l}{W3g} = 3.0\frac{\left(1-\frac{h}{hb}\right)\left[\left(\frac{hb}{h}\right)\left(\frac{\alpha 1b}{\alpha 1}\right)^2 - 1\right]\sqrt{\left(\frac{\rho lh}{\rho ghb}\right)\left(1-\left(\frac{hb}{D}\right)^2\right)}}{\left(\frac{hb}{d}\right)\left(0.22\frac{hb}{d}+1\right)} \tag{4}$$

$$\alpha 1b = 1 - \frac{1}{\pi}\cos^{-1}\left[\frac{2hb}{D}-1\right] + \frac{2}{\pi}\left[\frac{2hb}{D}-1\right]\left[\frac{hb}{D}\left(1-\frac{hb}{D}\right)\right]^{1/2} \tag{5}$$

$$\frac{w_{3g}^2}{gd^5\,\rho G(\rho L-\rho G)} = K\left(\frac{hb}{d}\right)^3\left[0.22\left(\frac{hb}{d}\right)+1\right]^2\left[1-\left(\frac{hb}{d}\right)^2\right]^{-1} \tag{6}$$

This model considers the effect of the branch pipe size. Nevertheless, it is disfavored by the hypothesis-based, theoretically derived coefficient, which has not been experimentally validated.

In 2018, Lu et al. [18] established the onset liquid entrainment model and branch quality model on the basis of a large-scale branch pipe at multi-angles. Lu et al. [18] mainly focused on the establishment of liquid entrainment model and the comparison with previous models. He did not analyze the effect of various parameters on liquid entrainment and the entrainment occurrence mechanism. In order to supplement his study, I completed the experiment of liquid entrainment through a large-scale T-junction under the same experimental conditions. This paper focused on the quantitative and qualitative study on the influence factors of onset entrainment and steady-state entrainment through a multi-angle large-scale T-junction.

To conclude, previous research mainly highlighted the small-scale branch pipe ($d/D \leq 0.2$) entrainment process, accompanied by establishment of mature theoretical systems and prediction models. Nevertheless, insufficient attention has been paid to liquid entrainment in large-scale branch pipes with different angles. Therefore, it is of great theoretical and engineering significance to investigate liquid entrainment in large-scale branch pipes, and

Table 2
Overview of vertical up T-junction liquid entrainment.

References	d/D	Background	Year
Crowley [6]	0.083	SB-LOCA	1981
Schrock [12]	0.1, 0.062, 0.0039, 0.037	SB-LOCA	1986
Smoglie [13]	0.097, 0.058, 0.039, 0.03	SB-LOCA	1987
Maciaszek [14]	0.15	SB-LOCA	1990
Yonomoto [15]	0.2, 0.125, 0.059, 0.053	SB-LOCA	1991
Welter [16]	0.33	ADS-4	2004
Present	0.675	ADS-4	2018

explore influences of branch pipe angles.

Through precise measurements, visualization and quantitative analysis, this study aims to figure out impact factors of onset liquid entrainment and steady liquid entrainment through a large-scale branch ($0.33 < d/D < 1$) with a variety of angles ranging between 32.2° and 90°(Fig. 2).

2. Experimental system and data analysis

2.1. Experimental system

As shown in Fig. 3, the whole experimental loop is divided into three parts, namely, the air supply system, water supply system and weighing backwater system. The key equipment of the air supply system is an air compressor with an exhaust pressure. An E+H (Germany Endress+ Hauser company) air mass flow meter is used to measure the air flow through a pneumatic tube. The key equipment of the water supply system includes a pump and a liquid turbine flow converter. Water is connected to the experimental phase through the PPR pipe (polypropylene random pipe). The key equipment of the backwater system for weighing is a weigh scale. Besides, precise water level measurements are critical throughout the experiment, and accordingly a high-precision pressure differential transmitter is employed.

Based on the measurement range and precision of each parameter, the uncertainty of each measurement parameter can be obtained. The fluid temperature is measured by a Φ1 mm thermocouple. The uncertainty of thermocouple is 0.31 °C. The feedwater flow rate is measured by a turbine flowmeter; the air flow is measured by mass flowmeter. The uncertainties of turbine flowmeter and mass flowmeter are 0.012 m^3h^{-1},0.43 kgh^{-1} respectively. The liquid level is measured by the micro differential pressure transmitter and the uncertainty of the differential pressure transmitter is 0.64Pa. The quality of entrained liquid is measured by the weigh scale and the uncertainty of the weigh scale is 2.9g. The Froude number reflects the ratio of inertial force to gravity. It is the most important dimensionless parameter in the study of T-junction entrainment. The Froude number in the liquid entrainment can be expressed as follows:

$$Frg = \frac{16w_{3g}^2}{\rho g(\rho f - \rho g)g\pi^2 d^5} \tag{7}$$

where w_{3g} is the gas mass flow rate in the branch pipe.

Therefore, the relative uncertainty of the Froude number in the liquid entrainment is as follows:

$$\frac{\sigma Fr_g}{Fr_g} = \sqrt{\left(\frac{U_{B,G}}{w_{3g}}\right)^2} \tag{8}$$

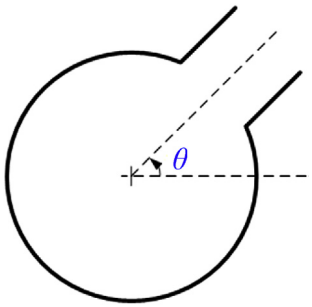

Fig. 2. Illustration of the branch angle.

It can be seen from the above formula that the maximum relative uncertainty of the Froude number in the liquid phase entrainment is 0.0022.

The branch quality is mainly related to h/h_b, and the calculation uncertainty of the liquid level h corresponding to a certain branch quality is related to the liquid phase mass flow rate w_{3f} and the vapor phase mass flow rate w_{3g}. Therefore, the calculation uncertainty of h is expressed as follows:

$$\delta H'_{w3g} = f\left(w_{3g} + \delta w_{3g}, w_{3f}\right) - f\left(w_{3g}, w_{3f}\right) \tag{9}$$

$$\delta H'_{w3f} = f\left(w_{3g}, w_{3f} + \delta w_{3l}\right) - f\left(w_{3g}, w_{3f}\right) \tag{10}$$

$$\delta H' = \sqrt{\delta H'^2_{w3g} + \delta H'^2_{w3f}} \tag{11}$$

Based on mathematical calculations, the above equation will produce a calculated uncertainty band that is different from the measurement uncertainty. Quantitatively, the calculation uncertainty is an order of magnitude smaller than the measurement uncertainty.

In order to observe the two-phase fluid flow in the experimental phase and analyze the entrainment mechanism, an organic glass tubing PMMA (polymethyl methacrylate) is used as the main part of the experiment, and the entrained fluid is separated at the end of the branch pipe through a gas-water separation device. The downstream of the main pipe is installed with two sluice valves, with the bigger one installed in the main pipe section to control the liquid level of the main pipe and the smaller one installed in the backwater pipe section. The upstream of the main pipe is made of organic glass materials. Visual observation method is employed when filling the water, which eventually forms a liquid seal to the main backwater section. Thus, the gas phase can be controlled to flow out from the branch pipe, and its flow can be determined.

Table 3 shows the range of the experimental instruments and equipment used. A large T tube is used in the experiment, with a main pipe inner diameter of 80 mm and a branch pipe inner diameter of 54 mm. Upstream of the branch pipe is 1700 mm and downstream of it is 800 mm. When air and water flow through the experimental section, air can entrain some water into the branch pipe, and they are separated in the gas-liquid separator. After being weighed, separated water is drained back into the tank. Water in the main pipe that has not been entrained into the branch pipe is returned to the tank through the downstream of the main pipe. All the air is propelled out of the branch pipe through the liquid seal towards the sluice valve of the downstream of the main pipe. In this context, the gas phase flow in the branch pipe is equal to the outlet flow of the air compressor.

2.2. Data analysis

According to previous research, the gas chamber height h is generally used to describe the liquid entrainment. It has not been well specified by most researchers that whether the upstream or the downstream liquid level of the main pipe should be used for h. Meng et al. [17] clearly indicated the downstream liquid level to be the one that should be used. They found that the upstream liquid level is similar to the downstream one under the condition of lower liquid level in the main pipe at the same Fr_g (Fig. 4), but they significantly differ from each other when the liquid level in the main pipe is high at the same Fr_g (Fig. 5) and the entrained droplets come from the downstream of the main pipe. Therefore, the downstream liquid level is believed to be one main factor affecting the liquid entrainment.

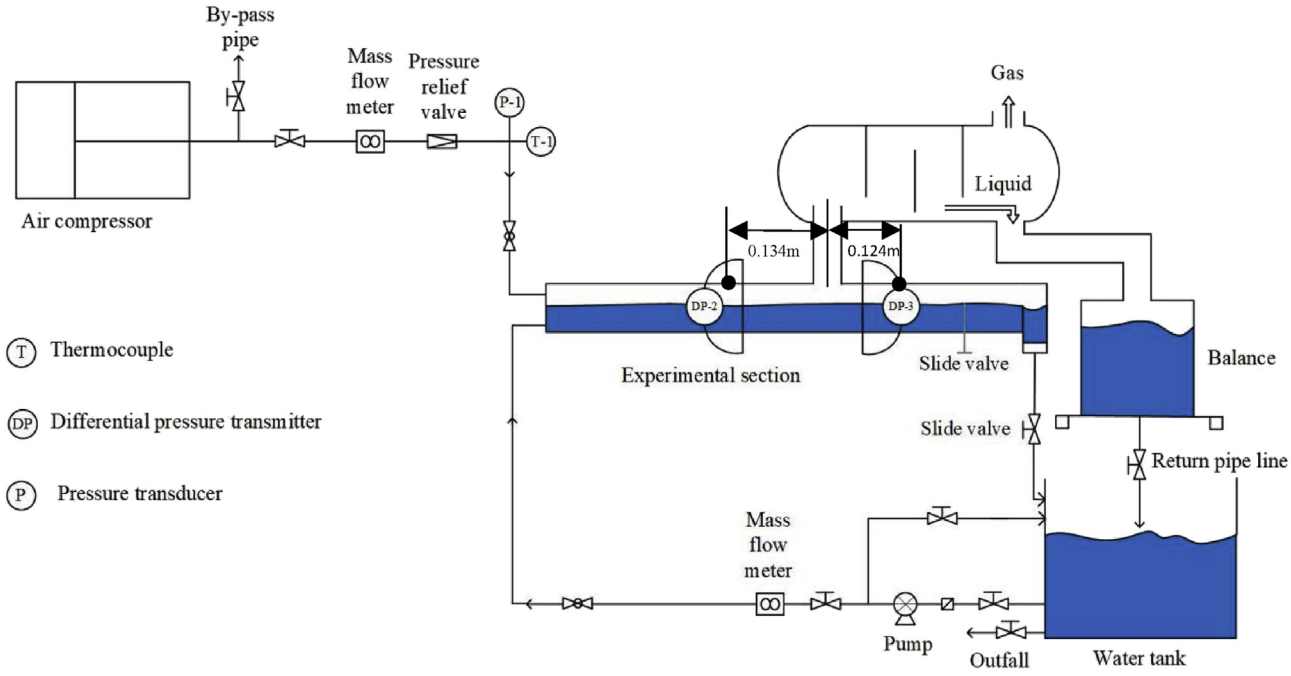

Fig. 3. Schematic diagram of the experimental system.

Table 3
Experimental parameters.

No.	Experimental Parameters	Range/Value	Unit
1	System pressure	Atmosphere	MPa
2	Gas temperature	Room	°C
3	Gas flow	0–0.056	kg/s
4	Liquid temperature	Room	°C
5	Liquid flow	0–0.28	kg/s

As an important factor for the onset of liquid entrainment, the critical height h_b is expressed by the dimensionless number h_b/d (Fig. 6). The timing when some droplets or the rising liquid film enter the branch pipe is defined as the onset liquid entrainment. For steady-state entrainment, h/d can be expressed by the gas chamber height.

3. Impact factors of the onset liquid entrainment

3.1. Branch pipe angles

Branch pipe angles 32.2°, 47.9°, 62.3° and 90° are employed for entrainment experiments under the same gas phase conditions. The visualization method is used for qualitative and quantitative analyses of their impacts on onset entrainment.

The resistance between the main pipe and branch pipe increases as Fr_g gradually decreases. At the same time, the liquid level fluctuates more violently until the liquid separates from the two-phase interface and is brought into the branch pipe by gaseous entrainment. That moment is defined as the onset of liquid entrainment. Corresponding experimental parameters are collected and visualized information is captured, for further quantitative and qualitative analysis of entrainment phenomenon. With changes in Fr_g of different gas phases, above steps are repeated, resulting in a series of liquid entrainment onset data corresponding to different branch angles and different Fr_g.

When the branch pipe is tilted at the vertically upward branch pipe of 90°, vortex appears above two-phase interfaces below the branch pipe inlet for all the experiments with different Fr_g, and liquid droplets are entrained into branch pipes spirally (Fig. 1(a–c)). In contrast, when the branch pipe is inclined (such as 32.2°), gas flow entrains liquid into the branch pipe by the continuous rising liquid film in all the experiments with different Fr_g (Fig. 1(d–f)). This is consistent with what Lee et al. [9] observed.

High liquid level in the main pipe becomes less needed for entrainment onset, as Fr_g increases. Thus, the onset height of the gas chamber will also rise accordingly (Fig. 7). With a smaller branch pipe angle, a corresponding larger Fr_g will appear under the same gas chamber height (Fig. 7), which shares consistency with

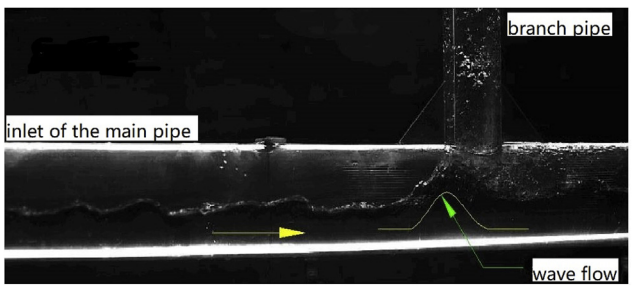

Fig. 4. Wave flow pattern corresponding to lower liquid level in the main pipe [17].

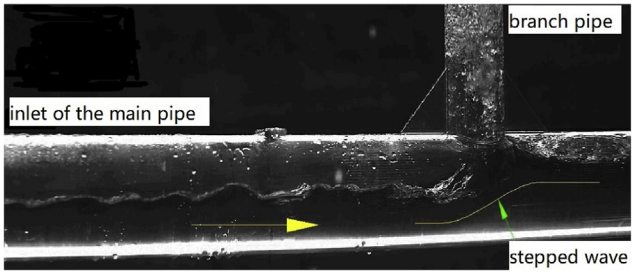

Fig. 5. Stepped wave pattern corresponding to higher liquid level in the main pipe [17].

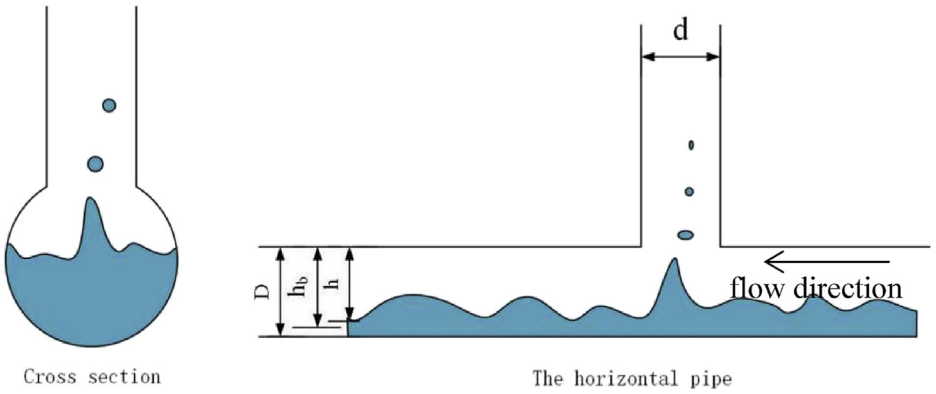

Fig. 6. Illusion of the gas chamber.

the experimental data obtained by Lee et al. [9] (Fig. 8).

The onset entrainment mainly depends on the upward inertial force applied by the transition from the gas phase to the liquid phase, which needs to overcome droplet gravity (Fig. 9). In the condition of constant gas chamber height and Fr_g, the angle between the inertial force applied by the gas phase to the liquid and the two-phase horizontal surface decreases, as the branch pipe angle decreases. Meanwhile, the inertial force of the liquid phase in the vertical direction $Fr_{g\perp}$ becomes smaller, whereas that in the horizontal direction $Fr_{g//}$is increased. Under these conditions, the entrainment requires a sufficient total inertial force. Fr_g should be large enough to ensure the onset liquid entrainment, as it reflects the inertial force/gravity ratio. At the same time, liquid along the horizontal direction will be affected, as the inertial force is markedly increased in the horizontal direction. As a summary, the two-phase interface starts to approach and climb along the main pipe wall, as the branch pipe angle decreases, which is eventually showed in the form of continuous liquid film (Fig. 1(d–f)).

As shown in Figs. 7 and 8, when the angles of the branch pipe are the same, the ordinates $Fr_g(\rho_g/\Delta\rho)^{\wedge 0.5}$ in our experiment is much smaller than that of Lee in the same critical gas chamber height. This phenomenon occurs mainly because of the difference between the branch and the main pipe size ($D_{Present}$ = 80 mm, $d_{Present}$ = 54 mm) and Lee's branch pipe and main pipe size (D_{Lee} = 184 mm, d_{Lee} = 16 mm or 24.8 mm). Lee's branch-main pipe has an inner diameter ratio of 0.13, which belongs to the small-scale pipe. In this experiment, the branch-to-main pipe inner diameter ratio is 0.675, which belongs to the large-scale pipe. The onset of

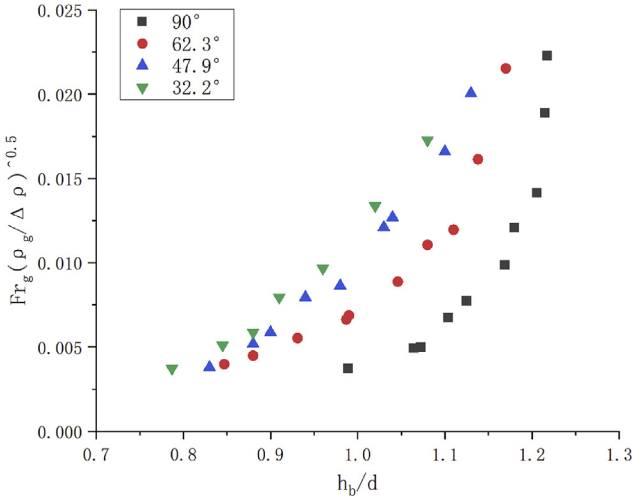

Fig. 7. Relationship between h_b/d and $Fr_g(\rho_g/\Delta\rho)^{\wedge 0.5}$ for onset liquid entrainment in branch pipes with certain angles.

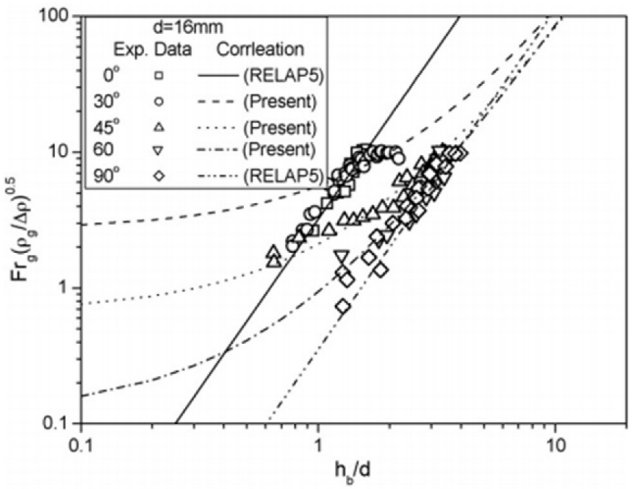

(a) d =16 mm

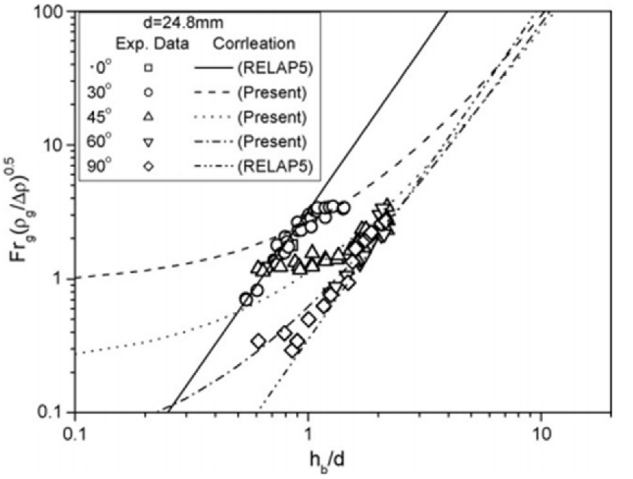

(b) d =24.8 mm

Fig. 8. Experimental data of Lee et al. [9].

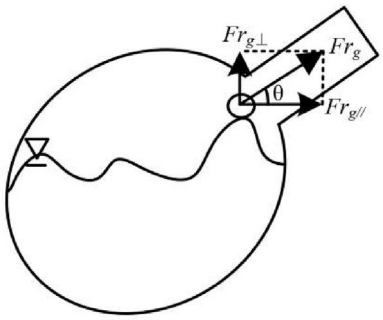

Fig. 9. Inertial force diagram of droplets.

entrainment occurs as a result of the inertial force overcoming the resistance. The resistance of the small branch is obviously larger than that of the large branch, so a larger inertia force is required to cause the onset of entrainment. Due to the influence of the pipe size, the ordinates of Lee is much larger than that of this experiment.

Based on above analysis, two main factors are demonstrated to be responsible for the onset of entrainment phenomenon under a certain gas chamber height, namely, the branch pipe angle and Fr_g. During the entrainment process, gas phase can provide the liquid phase with kinetic energy itself away from the two-phase interface. The branch pipe angle can affect the occurrence form of onset entrainment in a certain range. With the branch pipe angle becoming smaller, droplets that are initially entrained by gas-phase into the branch pipe, are gradually entrained by the continuous rising liquid film.

4. Impact factors of the steady-state liquid entrainment

4.1. Branch pipe angles

With the same w_{3g} and gas chamber height h/d, the branch quality x (i.e. branch quality is defined as the proportion of gas phase in the two-phase mass flow rate in the branch pipe) grows as the branch pipe angles increases (Fig. 10).

This can be attributed to the long axial distance of the branch pipe. Distance between the branch pipe outlet and the two-phase interface in the main pipe varies with the branch pipe angle (Fig. 11, $H_1>H_2$), which means varied branch pipe angle-dependent work against the gravity during liquid being entrained out of the branch pipe. Furthermore, turning over and falling back of liquid in the branch pipe is seen in the steady-state entrainment experiment.

A smaller branch pipe angle corresponds to a smaller distance between the branch pipe outlet and two-phase interface in the main pipe, and consequently a less amount of necessary work to overcome the gravity. In this context, almost all the continuous liquid phase is entrained out of the branch pipe (i.e. the branch quality x is lower). The phenomenon of liquid overturning and falling back in the branch pipe is low in frequency. As the branch pipe angle increases, the effective height of the branch pipe outlet from the two-phase interface in the main pipe also increases. Thus, entrained liquid needs to overcome more work of gravity, that is, the liquid is not easy to entrain out of the branch (i.e. the branch quality x becomes high). The phenomenon of liquid overturning and falling back in the branch pipe becomes severe. Therefore, with constant w_{3g}, the entrained liquid in the branch pipe per unit of time reduces as the branch pipe angle increases, which means growing the branch quality.

4.2. Gas chamber height and w_{3g}

With a certain gas chamber height, the branch quality basically decreases, as w_{3g} increases (Fig. 12). In other words, a larger gas phase flow rate corresponds to a larger liquid entrainment amount. However, for the 90° branch pipe, the steady-state entrainment phenomenon does not conform to the above trend when w_{3g} is around 0.54.

In order to find out the reason for the inapplicability of steady-state entrainment trend for 90° branch pipe, the gas chamber height is kept constant, whereas the gas phase flow is varied (Fig. 13). The amount of entrainment is found to first increase and then decrease with the increase of w_{3g}.

In addition, the gas chamber height in this study refers to the height of the downstream gas chamber in the main pipe (see Section 2.2), which means no consideration of the influence of the upstream gas chamber height. As shown in Fig. 14, the upstream gas chamber height gradually increases as w_{3g} increases, which gradually becomes to weaken the liquid entrainment. However, larger w_{3g} can enhance the liquid entrainment. For the steady

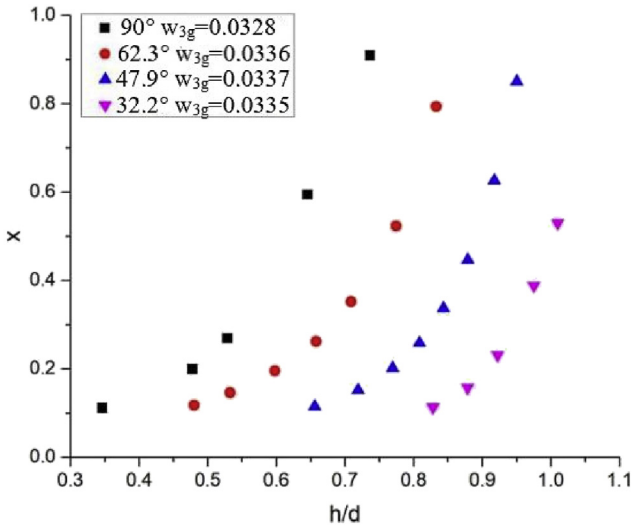

Fig. 10. Steady entrainment data for branch pipes with different angles.

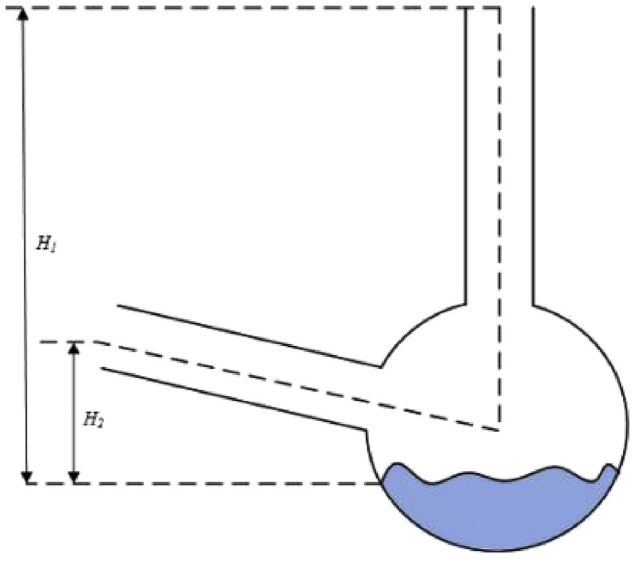

Fig. 11. Effective height of branch pipe outlet.

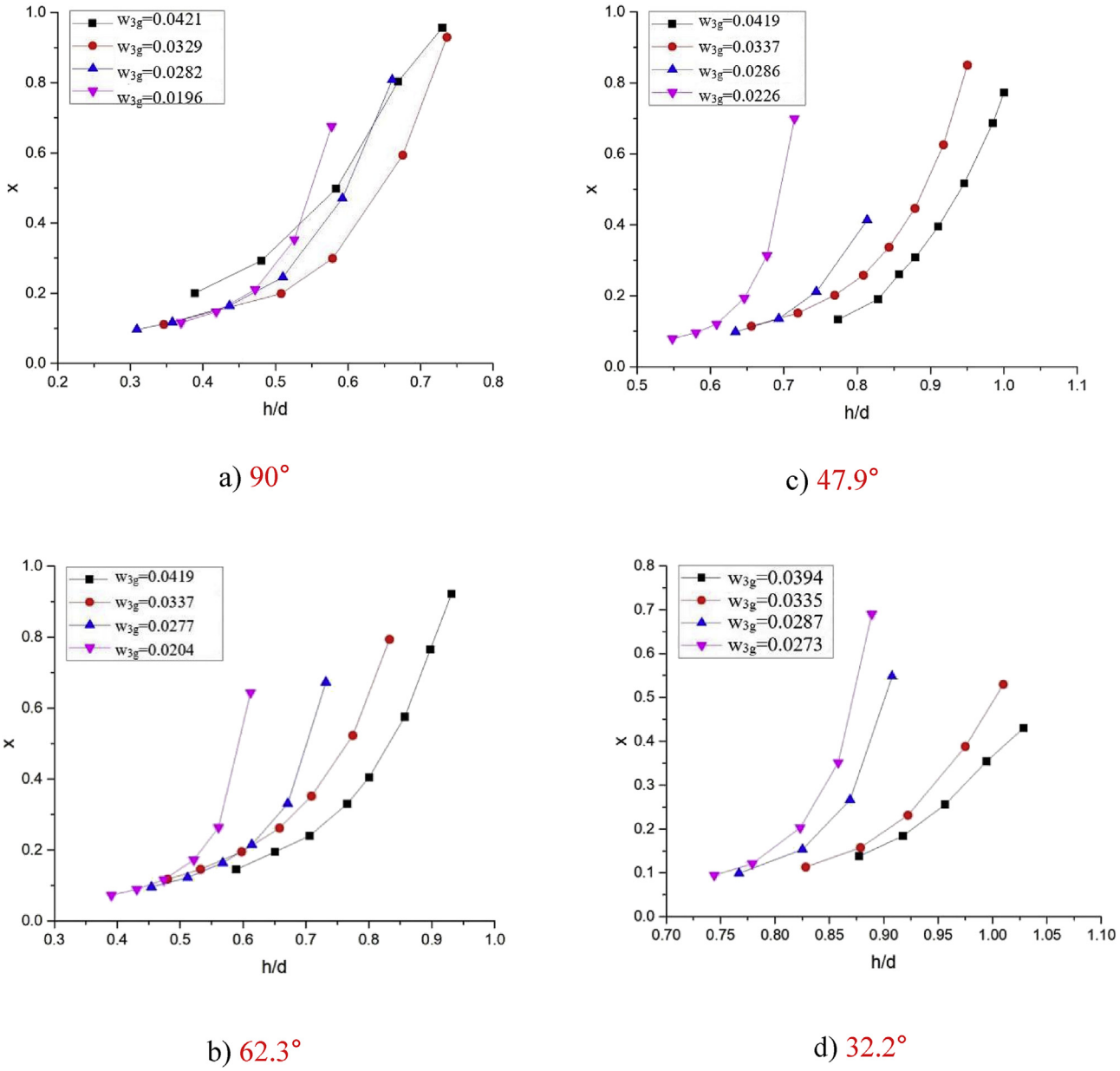

Fig. 12. Steady-state entrainment data for branch pipes with different angles.

entrainment process of the inclined branch pipe, with the same branch quality and w_{3g}, the gas chamber height increases as the branch pipe angle grows (Fig. 10), that is, the difference between upstream and downstream water level drops. Furthermore, entrainment forms of 32.2°,47.9° and 62.3° branch pipes, are significantly different from that of 90° branch pipe, and the upstream gas chamber height is large when w_{3g} is large. At that time, the horizontal component of the inertial force drives the liquid phase to accumulate toward the entrainment zone on the inclined side of the branch pipe. Therefore, the upstream gas chamber height has little influence on the entrainment, and consequently there is no violation of the entrainment model.

5. Conclusions

This study carries out experimental and theoretical research on the large-scale air-water T-junction experimental bench, aiming to qualitatively and quantitatively investigate effects of branch pipe angles (32.2°, 47.9°, 62.3° and 90°) on the onset of entrainment and steady-state entrainment. Following conclusions are drawn:

(1) The onset liquid entrainment arises earlier as the branch pipe angle increases. However, for the steady entrainment process, liquid entrainment intensity becomes weaker as the branch angle increases.
(2) For different branch pipe angles, there are two different onset entrainment forms. namely entrainment of droplets by the gas phase and that by the rising liquid film.
(3) For the 90° branch pipe with a constant gas chamber height, the entrainment amount first increases and then decreases, as w_{3g} grows. In constant, for the 32.2°, 47.9° and 62.3° branch pipes, the entrainment amount increases as w_{3g} increases.

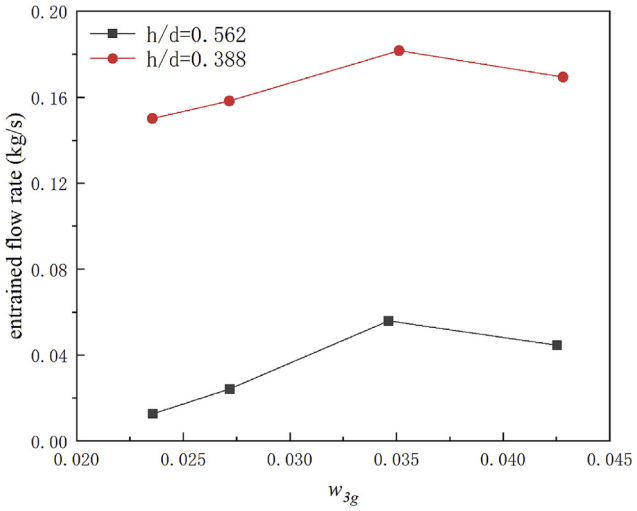

Fig. 13. Trend of varied gas flow with constant downstream liquid level.

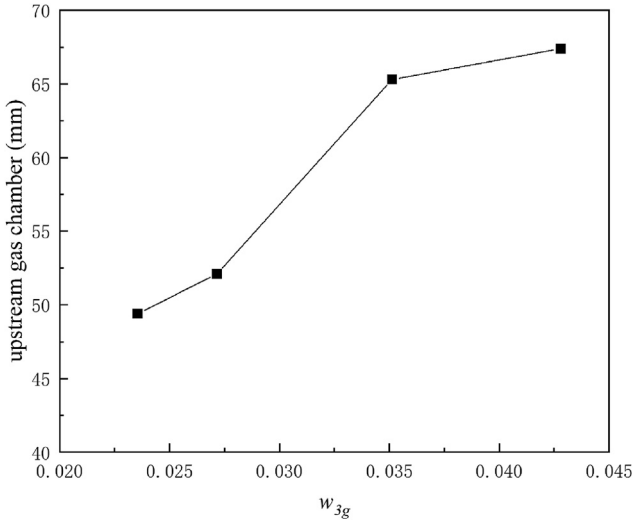

Fig. 14. Variation of the upstream gas chamber height with w_{3g}.

Acknowledgement

The work is supported by the National Natural Science Foundation of China (Grant Nos. 11605032 and 11605033), Fundamental Research Funds for the Central Universities of Ministry of Education of China (Grant No. GK2150260157) and Ph.D. Student Research and Innovation Fund of the Fundamental Research Funds for the Central Universities (3072019GIP1520). Yuenan Yang and Ningxin Gu contributed equally to this work.

Nomenclature

d	Branch pipe diameter
D	Main pipe diameter
Fr	Froude number
Fr_b	Froude number of continuous phase in the branch pipe
Fr_g	Froude number of gas phase in the branch pipe
$Fr_{g\perp}$	Froude number component of gas phase in the branch pipe in the vertical direction
$Fr_{g//}$	Froude number component of gas phase in the branch pipe in the horizontal direction
θ	Angle between the branch pipe and the horizontal direction
w_{3g}	Gas mass flow rate in the branch pipe
w_{3l}	Liquid mass flow rate in the branch pipe
ρ_g	Gas density
ρ_f	Liquid density
g	Gravitational acceleration
h	Distance between interface and branch centerline
h_b	Critical gas chamber height at the onset of liquid entrainment
x	Branch quality
H	Effective length of branch pipe
CANDU	Canadian Deuterium Uranium
ADS-4	Fourth Stage Automatic Depressurization System
PRHRS	Passive Residual Heat Removal System
LOCA	Loss of Coolant Accident
SB-LOCA	Small Break-Loss of Coolant Accident
OLE	Onset Liquid Entrainment

Appendix A. Supplementary data

Supplementary data to this article can be found online at https://doi.org/10.1016/j.net.2019.11.009.

References

[1] J. Kowalski, B. Hanna, Studies of two-phase flow distribution in a CANDU-type header/feeder system, in: Fourth International Topical Meeting on Nuclear Reactor Thermal-Hydraulics (NURETH-4). Proceedings, vol. 1, 1989.
[2] T.L. Schulz, Westinghouse AP1000 advanced passive plant, Nucl. Eng. Des. 236 (14) (2006) 1547–1557.
[3] W.W. Wang, G.H. Su, S.Z. Qiu, W.X. Tian, Thermal hydraulic phenomena related to small break LOCAs in AP1000, Prog. Nucl. Energy 53 (4) (2011) 407–419.
[4] N. Zuber, Problems In Modeling of Small Break LOCA. Technial Report, Nuclear Regulatory Commission, Washington, DC (USA), 1980. Div. of Reactor Safety Research.
[5] H. Rouse, Seven exploratory studies in hydraulics, Proceedings of ASCE 82 (4) (1956) 1–35.
[6] J. Crowley, Flow Visualization and Break Mass Flow Measurements in Small Break Separate Effects Experiments, EPRI, America, 1981.
[7] K.B. Welter, Liquid entrainment at an upward oriented vertical branch line from a horizontal pipe, Diss. Abstr. Int. (2002) 4–6.
[8] B.D. Chung, W.J. Lee, M. Hwang, Y.S. Bang, I.G. Kim, S.H. Ahn, RELAP5/MOD3 Horizontal Off-Take Model for Application to Reactor Headers of CANDU Type Reactors, Nuclear Regulatory Commission, U. S., 2010.
[9] J.Y. Lee, S.H. Hwang, M. Kim, G.C. Park, Onset condition of gas and liquid entrainment at an inclined branch pipe on a horizontal header, Nucl. Eng. Des. 237 (10) (2007) 1046–1054, https://doi.org/10.1016/j.nucengdes.2007.01.002.
[10] J.Y. Lee, G.S. Hwang, M. Kim, H.C. NO, Experimental analysis of off-take phenomena at the header–feeder system of CANDU, Ann. Nucl. Energy 33 (1) (2006) 1–12.
[11] J.T. Bartley, H.M. Soliman, G.E. Sims, Experimental investigation of the onsets of gas and liquid entrainment from a small branch mounted on an inclined wall, Int. J. Multiph. Flow 34 (10) (2008) 905–915.
[12] V.E. Schrock, S.T. Revankar, R. Mannheimer, Small Break Discharge the Roles of Vapor and Liquid Entrainment in a Stratified Two-phase Region Upstream of the break[R], Nuclear Regulation Commission, America, 1986.
[13] C. Smoglie, J. Reimann, U. Müller, Two phase flow through small breaks in a horizontal pipe with stratified flow, Nucl. Eng. Des. 99 (1987) 117–130.
[14] T. Maciaszek, J.C. Micaelli, CATHARE phase separation modeling for small breaks in horizontal pipes with stratified flow, Nucl. Eng. Des. 124 (3) (1990) 247–256.
[15] T. Yonomoto, K. Tasaka, Liquid and gas entrainment to a small break hole from a stratified two-phase region, Int. J. Multiph. Flow 17 (6) (1991) 745–765.
[16] K.B. Welter, Q. Wu, Y. You, K. Abel, D. McCreary, S.M. Bajorek, S.M. Reyes, Experimental investigation and theoretical modeling of liquid entrainment in a horizontal tee with a vertical-up branch, Int. J. Multiph. Flow 30 (12) (2004) 1451–1484.
[17] Z. Meng, B. Dong, L. Wang, X. Fu, W. Tian, Y. Yang, G. Su, Experimental research of liquid entrainment through ADS-4 in AP1000, Ann. Nucl. Energy 72 (2014) 428–437, https://doi.org/10.1115/ICONE22-30245.
[18] Z. Lu, Z. Meng, N. Gu, et al., Development of correlations for liquid entrainment through a large-scale inclined branch pipe connected to the main horizontal pipe, Experimental Thermal and Fluid Science 96 (2018) 128–136.